7th International Conference on Debris-Flow Hazards Mitigation

Numerical simulation for evaluating the phase-shift of fine sediment in stony debris flows

Taro Uchida[a,*], Yuki Nishiguchi[b], Brian W. McArdell[c] and Yoshifumi Satofuka[d]

[a]*National Institute for Land and Infrastructure Management, 1 Asahi, Tsukuba, Ibaraki 305-0804, Japan*
[c] *CTI Engineering, Co., Ltd., 1047-27,Onigakubo,Tsukuba, Ibaraki 300-2651, Japan*
[c] *WSL Swiss Federal Research Institute, CH-8903, Birmensdorf, Switzerland*
[c] *Ritsumeikan University, Kusatsu, Shiga, 525-8577, Japan*

Abstract

To predict hazard-endangered areas and debris-flow velocity, a variety of physically-based numerical simulation models have been developed. In these models, the relatively large sediment particles such as boulders move as a laminar flow, but the interstitial fluid between sediments behaves like a turbulent flow. Moreover, several recent models assumed that fine sediments act as a fluid. This behavior of fine sediment is referred to as the "phase-shift" of fine sediment. However, because it is difficult to observe the phase-shift of fine sediment in the field, adequate data on the phase-shift of debris flow are still lacking. In the last two decades, intensive monitoring for debris flow has been conducted all over the world, and observations have dramatically increased. For example, in the Illgraben catchment, Switzerland, observations of bulk density, pore pressure, flow depth, front velocity, and temporal and spatial patterns of erosion due to debris flows are available. So, we used these data for model input conditions. We applied the numerical simulation model Kanako-LS to evaluate the phase-shift concept for describing a variety of debris flow properties and behaviors at the Illgraben, Switzerland. Here we successfully describe a variety of observed debris flow behaviors, such as erosion and deposition pattern and shape and velocity of debris-flow fronts. However, if we ignored effects of phase-shift, the deposition volume was overestimated and flow velocity was underestimated.

Keywords: debris-flow; numerical simulation; input condition; hazard map; Aranayake disaster

1. Introduction

Stony (boulder-rich) debris flow have been described as consisting of two phases, the fluid and solid phase (e.g., Takahashi, 1991). Some researchers suggested that coarse sediment in stony debris flow move in a laminar manner, but interstitial fluid between sediment behaves like a turbulent flow (e.g., Takahashi, 1991). If a grain remains suspended for a period of time that exceeds the duration of a debris flow as a result of the viscous resistance of water only, it may act as part of the fluid (e.g., Iverson, 1997). In this study, this behavior of the fine sediment refers to "phase-shift" of fine sediment.

It has been considered that all of sediments often behave likes fluid in mud flow and rock avalanches (e.g., Hunger and Evans, 2004; Hotta and Miyamoto, 2008). Moreover, several researchers proposed two layers (i.e., the liquefied layer at the bottom and the solid layer at the surface flow) concept to describe long runout landslide (e.g., Iverson et al., 2015). This concept also hypothesized that all of sediments in bottom layer should be liquefied. In contrast to these concepts, we assumed that a part of sediments move as fluid and mixed two phases, solid and fluid, in the same layer.

The phase-shift of fine sediment might enhance the fluidity of debris flow due to reducing grain contact forces (e.g., Iverson and George, 2014; Iverson et al., 2010; de Haas et al., 2015). Moreover, it can be thought that the phase-shift of fine sediment increases the mass density of the interstitial fluid and enhances the transport capacity of stony debris flows (e.g., Nishiguchi et al., 2011). This effect of fine sediment on debris flow transport capacity has been tested in laboratory experiments. These experiments have shown that the greatest sediment transport capacity occurs in the

* Corresponding author e-mail address*: uchida-t92rv@mlit.go.jp*

debris flows that contain fine sediment (e.g., Hotta et al., 2013). Furthermore, several numerical simulation models describing fine sediment as fluid have been proposed (e.g., Nishiguchi et al., 2011; Uchida et al., 2013; Iverson and George, 2014).

However, previous numerical simulations mainly focused on only debris-flow travel distance and/or erosion and deposition patterns, because of lack of field data. Thus, effects of a phase-shift on flow properties, such as flow velocity, have not been fully examined. The objective of this study is to test effects of phase-shift on erosion/deposition patterns and flow velocity of debris flows by composing data from observation stations with simulation results. Herein, we applied a numerical simulation that included effects of phase-shift for describing not only erosion and deposition patterns, but also flow velocity and sediment concentration of debris flow in Illgraben, Switzerland, where one of most intensive debris flow monitoring sites in the world (e.g., McArdell et al., 2007; 2016; Berger et al., 2011).

2. Methods

2.1. Study site and data

The Illgraben catchment is located in southwest Switzerland. The active part of the catchment on the north face of Illhorn mountain has an area of 4.5 km^2 and is underlain by sedimentary rocks which weather to produce quartzite and dolomite boulders up to several meters in diameter, as well as some clay-size particles. The Illgraben debris-flow observation station was installed in 2000 to monitor debris flow activity. The station includes a large force plate (McArdell et al., 2007) that was installed at check dam 29 (Fig. 1). The force plate consists of a 2-m long, 4-m wide, three ton steel structure, installed flush with the base of the concrete check dam, which has a trapezoidal cross-sectional shape. A normal force transducer is installed under each corner and the forces are summed and recorded at 2 kHz. A laser sensor mounted on the road bridge above the force plate measures the distance to the top of the flow. McArdell et al. (2007) calculated the bulk density of debris flows using data of normal stress and flow depth. Furthermore, Berger et al. (2011) observed timing of erosion at the riverbed about 90 m upstream from the check dam 29.

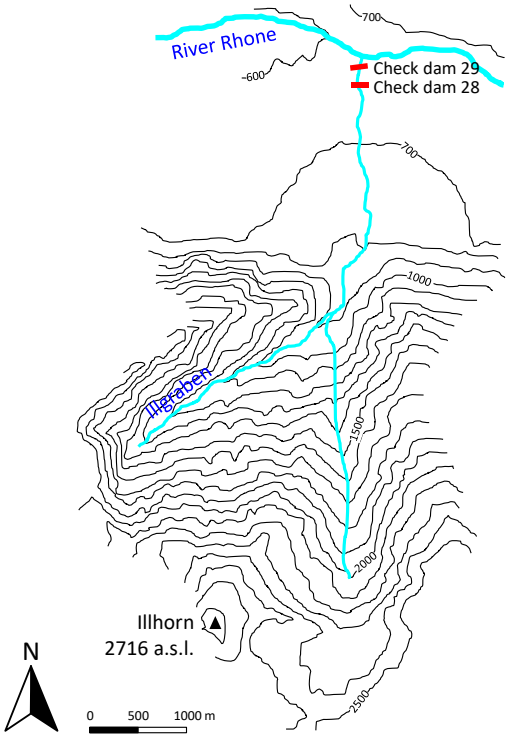

Fig. 1. Topographic map of Illgraben, Switzerland.

Many debris flows have been observed in Illgraben (e.g., McArdell et al., 2007; 2016; Berger et al., 2011). In this study, we focused on a debris flow that occurred on 1 July, 2008, because it is one of the most well-documented debris flows at the site to date. For 2008 debris flow, Berger et al. (2011) reported the peak flow discharge of 89 m^3/s at check dam 29. Observed bulk density ranged from 1200 to 2000 kg/m^3 (Berger et al., 2011). Berger et al. (2011) indicated that averaged density for the front part of debris flow (i.e., from the front arrival to 25 s after it) was relatively high, around 1800 kg/m^3. The bulk density of the debris flow tail (i.e., about 100 s after the front arrival) was about 1300 kg/m^3. The width of channel where erosion or deposition occurred ranged from 6 to 16 m.

2.2. Numerical simulation model

We applied our original 1D numerical simulation model, Kanako-LS, which was developed to include the process of phase shift (Uchida et al., 2013). The Kanako-LS model was based on the Kanako model developed by Nakatani et al. (2007) who modelled debris-flow properties, such as equilibrium concentration (i.e., the concentration that results in neither erosion of the bed nor deposition onto the bed), riverbed shear stress, and erosion and deposition rates using Takahashi's stony debris-flow theories (see Takahashi, 1991).

In Kanako-LS, the effect of "phase-shift" on debris-flow dynamics was modelled. We assumed that sediments can be classified into two groups (fine and coarse) on the basis of sediment diameter, and defined the critical diameter of the sediment (D_c) as the smallest diameter that behaves as a solid. That is, they proposed that sediments larger than D_c move as solids, while those smaller than D_c behave as fluids. So, sediment concentration for all sediments (C_s), i.e., coarse and fine sediments was described by coarse sediment concentration (C_c) and fine sediment concentration (C_f) as follow.

$$C_s = C_c + C_f \tag{1}$$

Moreover, we assumed that the mass density of interstitial fluid (ρ) can be described as

$$\rho = \sigma \frac{C_f}{1-C_c} + \rho_w \left(1 - \frac{C_f}{1-C_c}\right) \tag{2}$$

where σ is the mass density of the sediment and ρ_w is the mass density of clear water.

In Kanako-LS, the continuity equations for the total volume of debris flow and the entrained (removable) bed sediment are

$$B\frac{\partial h}{\partial t} + \frac{\partial uhB}{\partial x} = iB \tag{3}$$

$$\frac{\partial z}{\partial t} + i = 0 \tag{4}$$

where h is the flow depth, u is the flow velocity B is the flow width, x is the horizontal distance, t is time, i represents the erosion and deposition velocity, and z is the height of the riverbed. Moreover, two continuous equations for fine and coarse sediments were derived.

Erosion

$$B\frac{\partial C_c h}{\partial t} + \frac{\partial C_c uhB}{\partial x} = iC_{*ic}B \tag{5}$$

$$B\frac{\partial C_f h}{\partial t} + \frac{\partial C_f uhB}{\partial x} = iC_{*if}B \tag{6}$$

Deposition

$$B\frac{\partial C_c h}{\partial t}+\frac{\partial C_c uhB}{\partial x}=iC_{*dc}B \quad (7)$$

$$B\frac{\partial C_f h}{\partial t}+\frac{\partial C_f uhB}{\partial x}=iC_{*df}B \quad (8)$$

where C_{*ic} and C_{*if} are the concentrations of coarse and fine sediments in the initial mobile layer of the riverbed, respectively, and C_{*dc} and C_{*df} are the concentrations of coarse and fine sediments in the deposited layer of the riverbed, respectively.

We also applied the equations 9 and 10 for calculation of erosion and deposition rate respectively.

$$i=\delta_e\frac{C_\infty-C_c}{C_{*_i}-C_\infty}\frac{q}{d} \quad (9)$$

$$i=\delta_d\frac{C_\infty-C_c}{C_{*_d}}\frac{q}{d_c} \quad (10)$$

where δ_e and δ_d is the coefficient for the erosion and deposition velocity, respectively, C_{*i} is the sediment concentration in the initial entrained (removable) bed sediment, q is the flow rate per unit width, d is the representative sediment, including both coarse and fine sediments, diameter of riverbed, and d_c is the representative sediment diameter of coarse sediments.

We used three different equilibrium sediment concentration theories in terms of water surface gradient. We used the debris-flow theory for steep water surface, the sediment sheet flow theory for intermediate gradient water surface, and the bedload theory for gentle water surface (Uchida et al., 2013).

The momentum equation adopted is the same as that used in the original Kanako scheme

$$\frac{\partial u}{\partial t}+u\frac{\partial u}{\partial x}=-g\frac{\partial H}{\partial x}-\frac{\tau_h}{\rho h} \quad (15)$$

where H is the height of the water surface ($H = z + h$), g is the gravitational acceleration, and τ_h is the riverbed shearing stress. Based on the original Kanako scheme, we used three different flow resistance theories in terms of flow conditions to calculate the riverbed shearing stress (τ_h) (Uchida et al., 2013). We defined three flow conditions, as debris flow, sediment sheet flow, and ordinary turbulent water flow. We classified these flow conditions on the basis of the coarse sediment concentration (C_c).

2.3. Parameter setting

In this study, we simulated for the section between check dams 28 and 29, because detailed data about erosion and deposition patters reported by Berger et al. (2011) were available. We assumed the input hydrograph and bulk density at check dam 28 should be similar to observed hydrograph and bulk density at check dam 29, since the distance between check dams 28 and 29 is only 140 m and erosion and deposition between check dams 28 and 29 was not obvious. Based on the observed flow depth at check dam 29, we assumed a triangle shape as input hydrograph at the check dam 28. We set the duration of debris flow at 3000s and the peak discharge at 89 m^3/s, which appeared 21s after the front of debris flow.

Based on the observations of Berger et al. (2011), we set three bulk densities (ρ_m) as the averaged density of tail part of flow (1300 kg/m^3), entire debris flow (1500 kg/m^3) and the front part (1800 kg/m^3), respectively. In this study, we ignored the temporal change in bulk density at check dam 28. We set bulk densities of water and sediment at 1000 and 2600 kg/m^3, respectively, and we fixed the total sediment concentration, including both coarse and fine sediments, at 18.8, 31.3, and 50 % for ρ_m=1300, 1500 and 1800 kg/m^3, respectively (Table 1).

We did not have data on ratio of fine sediment that was present in the fluid phase. Thus, we simply set two phase-shift ratios, i.e., the ratio of phase-shifted fine sediment volume to total sediment volume (Table 1). In cases 1a-c, we assumed that effects of phase-shift were negligible. So, we considered that all of sediment behaved as solid phase (coarse sediment). In cases 2a-c, we assumed that 70 % of sediment phase-shifted and behaved as fluid phase. Other parameter values are summarized in Table 2.

Table 1. Numerical simulation cases

Case	Bulk density [kg/m^3]	C_s	PR	C_c	C_f	ρ [kg/m^3]	C_f'
Case 1a	1300	0.188	0.000	0.188	0.000	1000	0.000
Case 1b	1500	0.313	0.000	0.313	0.000	1000	0.000
Case 1c	1800	0.500	0.000	0.500	0.000	1000	0.000
Case 2a	1300	0.188	0.700	0.056	0.132	1223	0.139
Case 2b	1500	0.313	0.700	0.094	0.219	1387	0.242
Case 2c	1800	0.500	0.700	0.150	0.350	1659	0.412

C_s; total sediment, including both coarse and fine, concentration, PR Phase-shift ratio (=C_f/C_s),
C_c; coarse sediment concentration, C_f Fine sediment concentration,
ρ ; density of interstitial fluid, C_f' Fine sediment concentration in interstitial fluid (=C_f/(1-C_c))

Table 2. Parameter values

Parameters	Symbol	Value	Unit
Mass density of pure water	ρ_w	1000	kg m^{-3}
Mass density of sediment	σ	2600	kg m^{-3}
Sediment concentrations in the initial mobile layer of the riverbed	C_{*i}	0.65	-
Sediment concentrations in the deposited layer of the riverbed	C_{*d}	0.65	-
Coefficient for erosion velocity	δ_e	0.0007	-
Coefficient for deposition velocity	δ_d	0.05	-
Friction angle of sediment	$\tan\phi$	0.7	-
Gravitational acceleration	g	9.8	m s^{-2}
Manning's coefficient	n	0.045	s m$^{-1/3}$
Depth of removable materials on initial riverbed		1.3	m
Time step for calculation	-	0.005	s

3. Results

3.1. Erosion and deposition pattern

Berger et al. (2011) conducted topographic survey before (17 June, 2008) and after (4 July, 2008) our studied debris at the section between check dams 28 (upstream) and 29. This survey showed that erosion dominated at the upper section of survey area (downstream of check dam 28), while deposition occurred at the lower section (upstream of check dam 29) (Fig. 1). Maximum measured erosion and deposition depths were around 1.1 and 0.9 m.

In contrast, if we assumed no phase-shift conditions (Cases 1), obvious deposition occurred at the section between check dams 28 and 29 (Fig. 2). Deposition volume became large, because the input sediment concentration became large (Fig.2a). Although if we input the lowest observed sediment concentration (case 1a), the deposition depth was around 12 m at the downstream of check dam 28, although the observed maximum deposited depth was 0.9 m. In case 1c, the riverbed was elevated more than 30 m at the downstream of check dam 28.

In the phase-shift case, the deposition depth became dramatically smaller. In case 2a (C_s=0.188), deposition occurred in almost the entire section. In the lower part of the section (i.e., more than 90 m away from the check dam), the deposition depth was relatively large (0.5-0.8 m), compared with the upper part (~0.3 m). While, in case 2b (C_s=0.313), the deposition was dominant in the lower part of the section, but the erosion was dominant in the upper section. In case 2c (C_s=0.500), the riverbed was eroded in the entire section. The erosion depth in the upper part was around 0.4-0.7m, while, in the lower part was around 0.1-0.4 m. The patterns from case 2c are well agreed well with

the observations. In conclusion, we successfully model the observed erosion and deposition pattern, although we have to fine tune the phase-shift ratio.

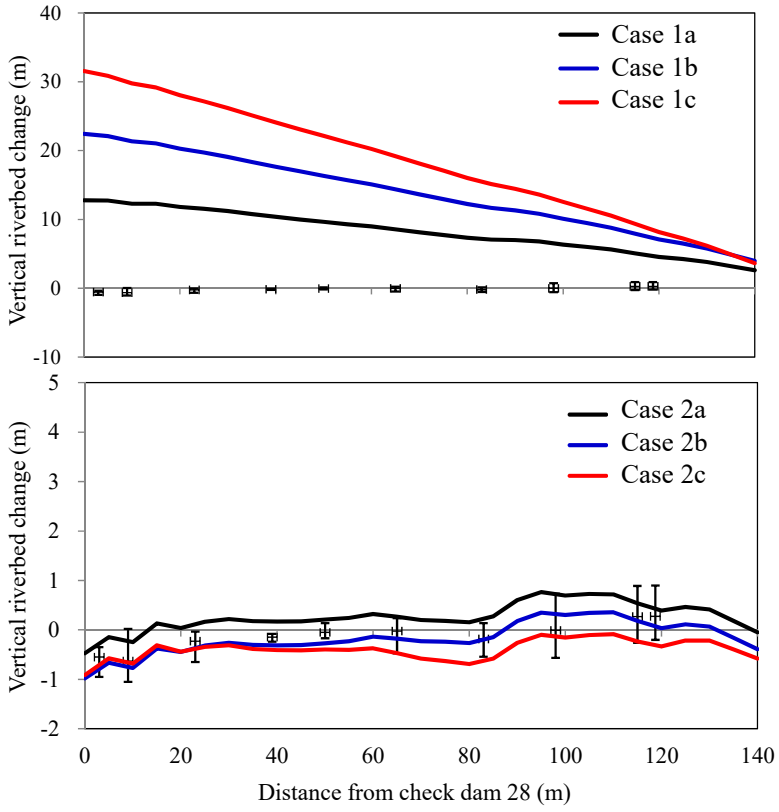

Fig. 2. Simulated elevation change due to debris flow. Positive and negative change indicate deposition and erosion, respectively. Observed data were compiled based on the Figures 10 and 11 of Berger et al. (2011). Plots indicate mean value and the upper and lower ends of error bars indicate maximum and minimum on the cross sections.

3.2. Front shape and velocity of the debris flow

Berger et al. (2011) showed temporal change in longitudinal profile of the surface of the debris flow immediately upstream of the front of debris flow at the section between check dams 28 and 29 (Fig. 1). They reported the longitudinal profile of debris flow front for 10 seconds after the front arrived at check dam 28. Thus, here we compared the calculated longitudinal profile of debris flow front with the observed profiles. Since the observed bulk density of the debris flow front ranged from 1700 to 2000 kg/m3, we focused on the cases that the bulk density was 1800 kg/m^3 (i.e., cases 1c and 2c) (Fig. 3).

The front velocity in case 2c is greater than that of case 1c, indicating that the front velocity increased with an increase in the phase-shift ratio. This suggests that the flow resistance became small as the phase-shift ratio became large (Fig. 3). Moreover, the calculated longitudinal surface angle of debris-flow front became gentle as the phase-shift ratio increased. The front velocity of phase-shift condition was 1.5 times greater than that of no phase-shift condition.

The front shape and velocity of case 2c agreed well with observations. However, if we ignored effects of phase-shift of fine sediment, the front height and velocity were underestimated (Fig. 3).

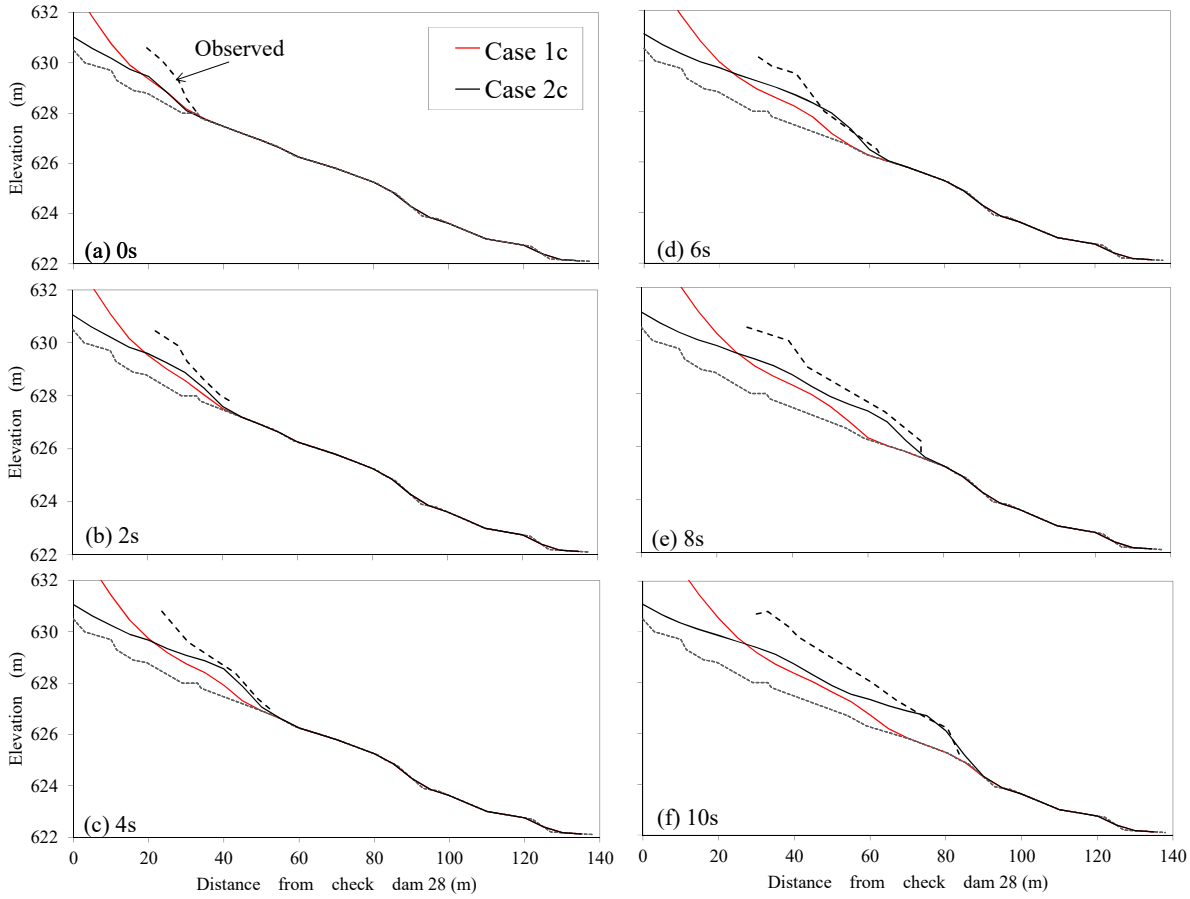

Fig. 3. Simulated front shape of debris flow. Observed data was compiled based on Figure 4 of Berger et al. (2011).

4. Discussion and conclusions

In this study, we test the applicability of numerical simulation models for describing not only erosion and deposition patterns, but also front shape and velocity and the effect of the phase-shift of fine sediment on deposition depth and flow velocity of the July, 2008 debris flow at Illgraben, Switzerland. We applied the numerical simulation model Kanako-LS to test the phase-shift concept on a well-documented dataset from the Illgraben debris-flow observation station. We successfully modeled the observed erosion and deposition pattern, and the front shape and velocity of the debris flow, although we have to fine tune the phase-shift ratio (i.e., ratio of fine sediment to the total sediment, which behaves as a fluid).

We showed that the phase-shift ratio has an extremely large impact on the erosion and deposition pattern. If we ignored effects of phase-shift, the deposition depth was more than 10 times larger than observed. This suggests that the effect of phase-shift on equilibrium concentration is very large. On the contrary, the influence of the phase-shift ratio on the on the front velocity was relatively small. When the phase shift was considered, the observed front velocity was 1.4 times larger than when the phase-shift effect was neglected. This suggests that the effect of phase shift on flow resistance is relatively small, but still significant.

Additionally, we showed that the numerical simulation of debris-flow runout could be effective for predicting not only erosion and deposition patterns, but also flow-front velocity. This demonstrates that numerical simulation of debris flow should be effective for prediction of not only potential affected area, but also the force acting on structures, such as houses, infrastructure, and structural countermeasures. If we don't have any ground truth data, we have to predict phase-shift ratio (e.g., Nishiguchi and Uchida, 2019). We consider that the phase-shift ratio should be controlled by both hydraulic condition of debris flow, such as flow depth etc. and particle size distribution of sediment

in debris flow. So, we need more study for clarifying relationship between the phase-shift ratio, hydraulic condition and particle size distribution.

References

Berger, C., McArdell, B.W., and Schlunegger, F., 2011, Direct measurement of channel erosion by debris flows, Illgraben, Switzerland: Journal of Geophysical Research-Earth Surface, v. 116, doi: 10.1029/2010JF001722.

de Haas, T., Braat, L., Leuven, J.R.F.W., Lokhorst, I.R., and Kleinhans, M.G., 2015, Effects of debris flow composition on runout, depositional mechanisms, and deposit morphology in laboratory experiments: Journal of Geophysical Research-Earth Surface, v.120, p.1949–1972, doi: 10.1002/2015JF003525.

Hotta, N., and Miyamoto, K., 2008, Phase classification of laboratory debris flows over a rigid bed based on the relative flow depth and friction coefficients: International Journal of Erosion Control Engineering, v.1, p.54-61, doi: 10.13101/ijece.1.54.

Hotta, N., Kaneko, T., Iwata, T., and Nishimoto, H., 2013, Influence of fine sediment on the fluidity of debris flows: Journal of Mountain Science, v.10, p.233-238, doi: 10.1007/s11629-013-2522-y

Hungr, O., and Evans, S., 2004, Entrainment of debris in rock avalanches: An analysis of a long run-out mechanism: Geological Society of America Bulletin, v.116, p.1240-1252, doi: 10.1130/B25362.1.

Iverson, R.M., 1997, The physics of debris flows: Reviews of Geophysics, v.35, p.245–296, doi: 10.1029/97RG00426

Iverson, R.M., Logan, M., LaHusen, R.G., and Berti, M., 2010, The perfect debris flow? Aggregated results from 28 large scale experiments, Journal of Geophysical Research-Earth Surface, v.115, doi: 10.1029/2009JF001514.

Iverson R.M., and George, D.L., 2014, A depth-averaged debris-flow model that includes the effects of evolving dilatancy. I. Physical basis: Proceedings of the Royal Society of London, Ser. A, v.470, doi: 10.1098/rspa.2013.0819

Iverson, R.M., George, D.L., Allstadt, K., Reid, M.E., Collins, B.D., Vallance, J.W., Schilling, S.P., Godt, J.W., Cannon, C.M., Magirl, C.S., Baum, R.L., Coe, J.A., Schulz, W.H., and Bower, J.B., 2015, Landslide mobility and hazards: implications of the 2014 Oso disaster: Earth and Planetary Science Letters, v.412, p.197-208, doi: 10.1016/j.epsl.2014.12.020.

McArdell, B.W., Bartelt, P., and Kowalski, J., 2007, Field observations of basal forces and fluid pore pressure in a debris flow: Geophysical Research Letters, v.34, L07406, doi: 10.1029/2006GL029183.

McArdell, B.W., 2016, Field measurements of forces in debris flows at the Illgraben: Implications for channel-bed erosion: International Journal for Erosion Control Engineering, v.7, 194-198, doi: 10.13101/ijece.9.194.

Nakatani, K., Satofuka, Y., and Mizuyama, T., 2007, Development of 'KANAKO', a wide use debris flow simulator equipped with GUI: Proceedings of 32nd Congress of IAHR, Venice, Italy, CD-ROM, 10p, A2, c-182.

Nishiguchi, Y., Uchida, T., Tamura, K. and Satofuka, Y., 2011, Prediction of run-out process for a debris flow triggered by a deep rapid landslide: Proceedings of 5th Debris Flow Hazard Mitigation Conference, p.477–485, doi: 10.4408/IJEGE.2011-03.B-053.

Nishiguchi, Y., and Uchida, T., 2019, Lonmg travel distance of landslide induced debris flow: Proceedings of 7th Debris Flow Hazard Mitigation Conference, (in this volume).

Takahashi, T., 1991, Debris flow. Balkema, Rotterdam, 165p.

Uchida, T., Nishiguchi, Y., Nakatani, K., Satofuka, Y., Yamakoshi, T., Okamoto, A., and Mizuyama, T., 2013, New Numerical Simulation Procedure for Large-scale Debris Flows (Kanako-LS): International Journal of Erosion Control Engineering, v.6, p.58-67, doi:. 10.13101/ijece.6.58